

Electronic supplementary materials

For: <https://doi.org/10.1631/jzus.A2300159>

Evolution mechanism and quantitative characterization of initial micro-cracks in marble under triaxial compression

Zhiliang WANG¹, Songyu LI¹, Jianguo WANG², Ao LI¹, Weixiang WANG¹, Chenchen FENG¹, Jingjing FU¹

¹School of Civil Engineering, Hefei University of Technology, Hefei 230009, China

²School of Mechanics and Civil Engineering, China University of Mining and Technology, Xuzhou 221116, China

S1 Marble material and experimental procedures

S1.1 Marble material

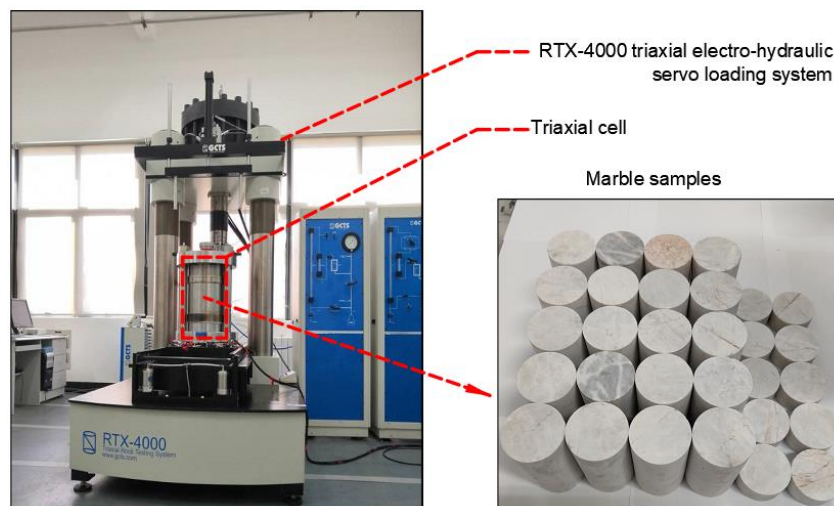


Fig. S1 Photos of triaxial compression device and marble samples

A series of triaxial tests were carried out on the RTX-4000 triaxial electro-hydraulic servo loading system at the China University of Mining and Technology (Fig. S1). The marble used in the test was taken from Jinping II Hydropower Station, Sichuan Province, China, and the average principal stress at the sampling site was between 35 and 50 MPa. X-ray diffraction (XRD) test results showed that the mineral composition of the marble material was mainly dolomite (69.31%), calcite (20.35%), and quartz (5.44%). Each marble sample was taken from the same rock block and processed into a standard cylinder with 50 mm in diameter and 100 mm in height. The sample was polished according to the recommendations of the International Society of Rock Mechanics (ISRM) until it met the test requirements (e.g., end face parallelism less than ± 0.05 mm) (Fairhurst and Hudson, 1999). A photo of marble samples is shown in Fig. S1.

S1.2 Experimental procedures

31 Before the triaxial compression experiment, the longitudinal wave velocity and density were
 32 measured for each sample. Based on the measurement results, the samples differing greatly from the
 33 average were discarded to eliminate the discreteness among the samples as far as possible. Among the
 34 samples in the triaxial compression test, the average wave velocity and density were 3700 m/s and 2800
 35 kg/m³, respectively. The detailed steps of the triaxial compression test and corresponding control
 36 conditions (confining pressure loading rate and axial pressure loading rate) are given in (Wang et al.,
 37 2022).

38
 39

$$\sigma_3 = 0 \text{ MPa}, \quad \varepsilon = (1 - 9.10 \times 10^{-4}) \frac{\sigma}{36817.90} + 9.10 \times 10^{-4} \left(1 - e^{-\frac{\sigma}{22.81}} \right), \quad (\text{S1})$$

$$\sigma_3 = 10 \text{ MPa}, \quad \varepsilon = (1 - 2.79 \times 10^{-4}) \frac{\sigma}{37029.14} + 2.79 \times 10^{-4} \left(1 - e^{-\frac{\sigma}{22.85}} \right), \quad (\text{S2})$$

$$\sigma_3 = 20 \text{ MPa}, \quad \varepsilon = (1 - 3.34 \times 10^{-4}) \frac{\sigma}{41081.38} + 3.34 \times 10^{-4} \left(1 - e^{-\frac{\sigma}{28.48}} \right), \quad (\text{S3})$$

$$\sigma_3 = 30 \text{ MPa}, \quad \varepsilon = (1 - 3.55 \times 10^{-5}) \frac{\sigma}{44940.03} + 3.55 \times 10^{-5} \left(1 - e^{-\frac{\sigma}{29.13}} \right), \quad (\text{S4})$$

$$\sigma_3 = 40 \text{ MPa}, \quad \varepsilon = (1 - 1.85 \times 10^{-4}) \frac{\sigma}{43163.70} + 1.85 \times 10^{-4} \left(1 - e^{-\frac{\sigma}{38.95}} \right), \quad (\text{S5})$$

$$\sigma_3 = 50 \text{ MPa}, \quad \varepsilon = (1 - 6.96 \times 10^{-5}) \frac{\sigma}{43110.75} + 6.96 \times 10^{-5} \left(1 - e^{-\frac{\sigma}{54.89}} \right). \quad (\text{S6})$$

40
 41
 42

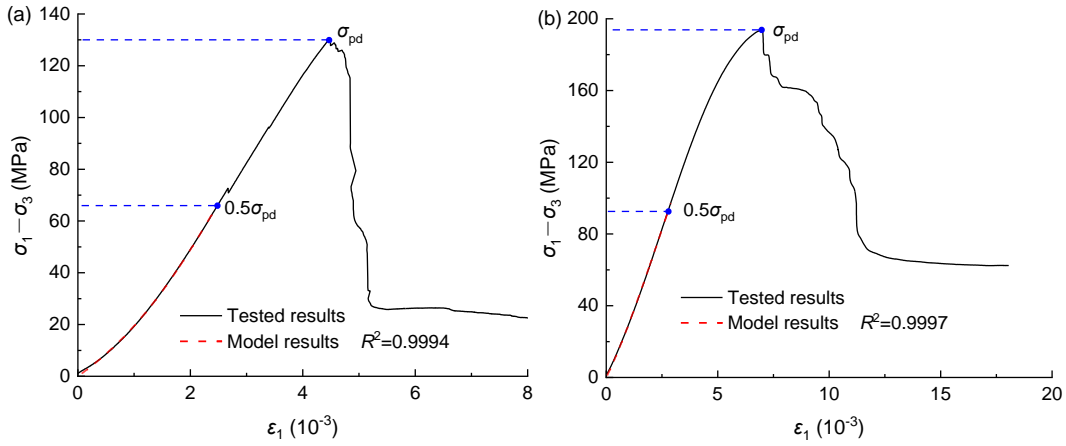
Table S1 Variation of deformation parameters for rock matrix and crack with confining pressure

σ_3 (MPa)	V_C/V	E_c (MPa)	E_m (GPa)	E_s (GPa)	μ_s
0	9.10×10^{-4}	22.81	36.82	33.33	0.34
10	2.79×10^{-4}	22.85	37.03	36.87	0.19
20	3.34×10^{-4}	28.48	41.08	40.18	0.15
30	3.55×10^{-5}	29.13	44.94	46.18	0.17
40	1.85×10^{-4}	38.95	43.16	42.33	0.17
50	6.96×10^{-5}	54.89	43.11	42.91	0.14

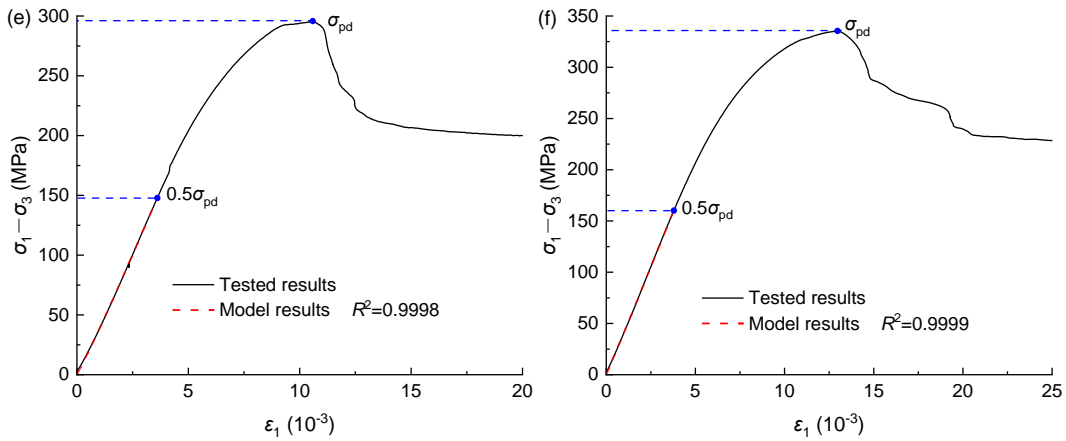
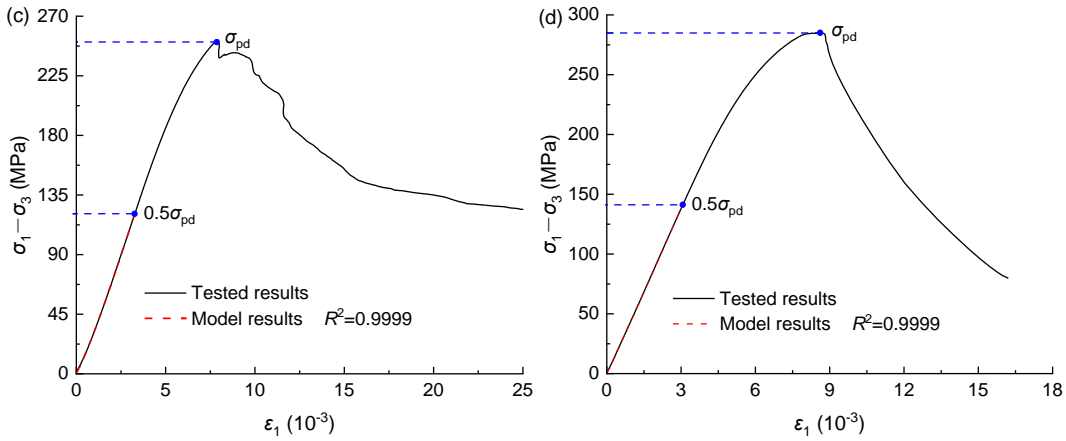
43
 44
 45

46 **S2 Comparison between the quantitative crack analysis model curves and marble test results**
 47
 48

49



50



51

52 **Fig. S2 Comparison between the quantitative crack analysis model curves and marble test results: (a) $\sigma_3 = 0$ MPa;**
 53 **(b) $\sigma_3 = 10$ MPa; (c) $\sigma_3 = 20$ MPa; (d) $\sigma_3 = 30$ MPa; (e) $\sigma_3 = 40$ MPa; (f) $\sigma_3 = 50$ MPa**

54

55 **S3 CT scanning of triaxial compression marble samples**

56

57 To explore the relationship between internal crack propagation and failure characteristics, CT
 58 scanning was performed on the samples (σ_3 was as taken as 0, 30, or 50 MPa) after the aforementioned
 59 triaxial compression experiment. A 3D reconstruction of sample failure was carried out, and sections of
 60 typical axial positions were selected to illustrate the internal failure characteristics. Typical axial section
 61 positions were taken as (diameter $d =$) 7, 14, 21, 28, 35, and 42 mm, respectively.

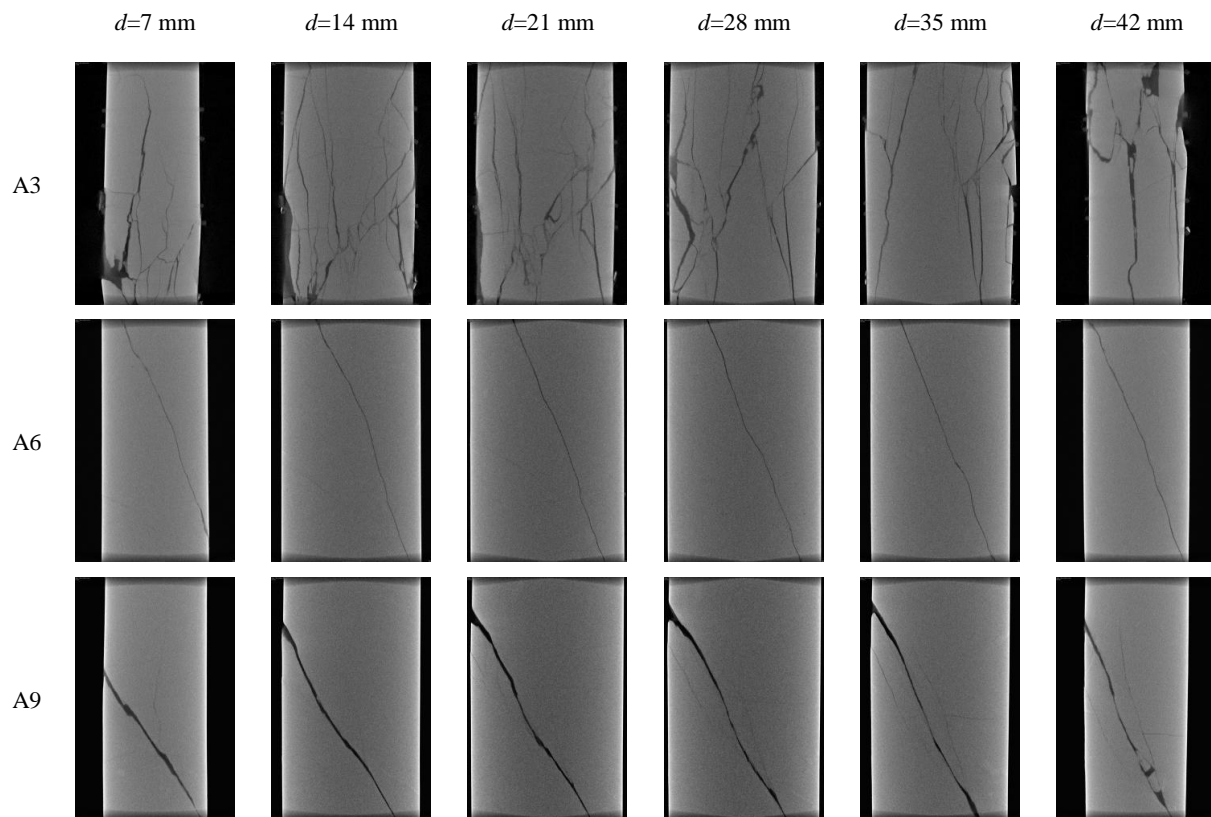


Fig. S3 CT scanning sections of triaxial compression marble samples with different axial positions

63

64

65 References

66 Fairhurst CE, Hudson JA, 1999. Draft ISRM suggested method for the complete stress–strain curve for intact

67 rock in uniaxial compression. *International Journal of Rock Mechanics and Mining Sciences*,

68 36(3):279-289.

69 Wang ZL, Li SY, Wang JG, et al., 2022. Mechanical behavior, mesoscopic properties and energy evolution of

70 deeply buried marble during triaxial loading. *International Journal of Damage Mechanics*,

71 31(10):1592-1612.

72